Swiss J Geosci (2017) 110:565–580
DOI 10.1007/s00015-017-0265-4

Reconciling late faulting over the whole Alpine belt: from structural analysis to geochronological constrains

Audrey Bertrand[1] · **Christian Sue**[2]

Received: 7 June 2016 / Accepted: 13 February 2017 / Published online: 1 March 2017

Abstract The significance of late-stage fracturing in the European Alps in a large geodynamic context is reappraised by studying brittle deformations over the entire belt. In the internal Western Alps, paleostress datasets display a major occurrence of orogen-parallel extension resulting in normal faulting and associated strike-slip mode. There the direction of subhorizontal extension rotates with the bending of the Alpine belt. In the Central Alps, paleostress tensors also indicate orogen-parallel extensional regimes, both in the Bergell area and the Lepontine Dome, where the brittle structures are associated with ductile structures related to the formation of large-scale upright folds that accommodate most of the collisional shortening due to the north-directed component of the movement of the South-Alpine indenter. This brittle deformation phase is of Miocene age and is coeval with the propagation of the Alpine front toward the external Alpine domains. In the Eastern Alps, brittle deformation of the Tauern Window displays an overwhelming occurrence of orogen-parallel normal faulting and associated strike-slip regimes again, which is inferred to be driven by lateral extrusion of the orogenic wedge toward the Pannonian basin, partly due to indentation on the Dolomites indenter. The major orogen-parallel extensional signal of the brittle Cenozoic deformations appears remarkably stable all over the internal Alps. Extensional brittle structures are part of a late phase of collisional deformation, during which the propagation of the Alpine front of the Western Alps and the northward movement of the Southern Alpine and the Dolomites indenters in the Central and Eastern Alps were accommodated by orogen-parallel extension in the inner zones, at the scale of the entire chain.

Keywords Structural analysis · Alpine belt · Late-stage faulting

1 Introduction

It is well constrained and largely accepted that the exhumation of the Alps results from the collision between European and Adriatic plates due to the relative northward movement of the Adriatic microplate (e.g. Termier 1903; Argand 1916, 1924; Dewey et al. 1973; Handy et al. 2010; Schmid and Kissling 2000; Schmid et al. 2017). However, late exhumation of the Alps differs significantly in terms of the sites of enhanced exhumation within the chain, both laterally and along strike. The actual shape and topography of the Alpine belt is related to tectonic, climatic and erosional processes. In the Late Eocene, the subduction of the Tethyan oceans beneath the Adriatic plate was followed by continent–continent collision inducing uplift and exhumation of the Western-Central Alps and the central part of the Eastern Alps (Dewey et al. 1989). The differences in buoyancy forces and flexural strengths between oceanic and continental lithosphere induced an Oligocene slab break-off (Von Blanckenburg and Davies 1995),

Editorial handling: S. Schmid.

Electronic supplementary material The online version of this article (doi:10.1007/s00015-017-0265-4) contains supplementary material, which is available to authorized users.

✉ Audrey Bertrand
audreybertran@gmail.com

[1] MTA-ELTE Geological, Geophysical and Space Science Research Group, Hungarian Academy of Sciences, 1/C Pázmány P. Sétány, Budapest 1117, Hungary

[2] CNRS-UMR6249, Bourgogne Franche-Comté University, Besançon, France

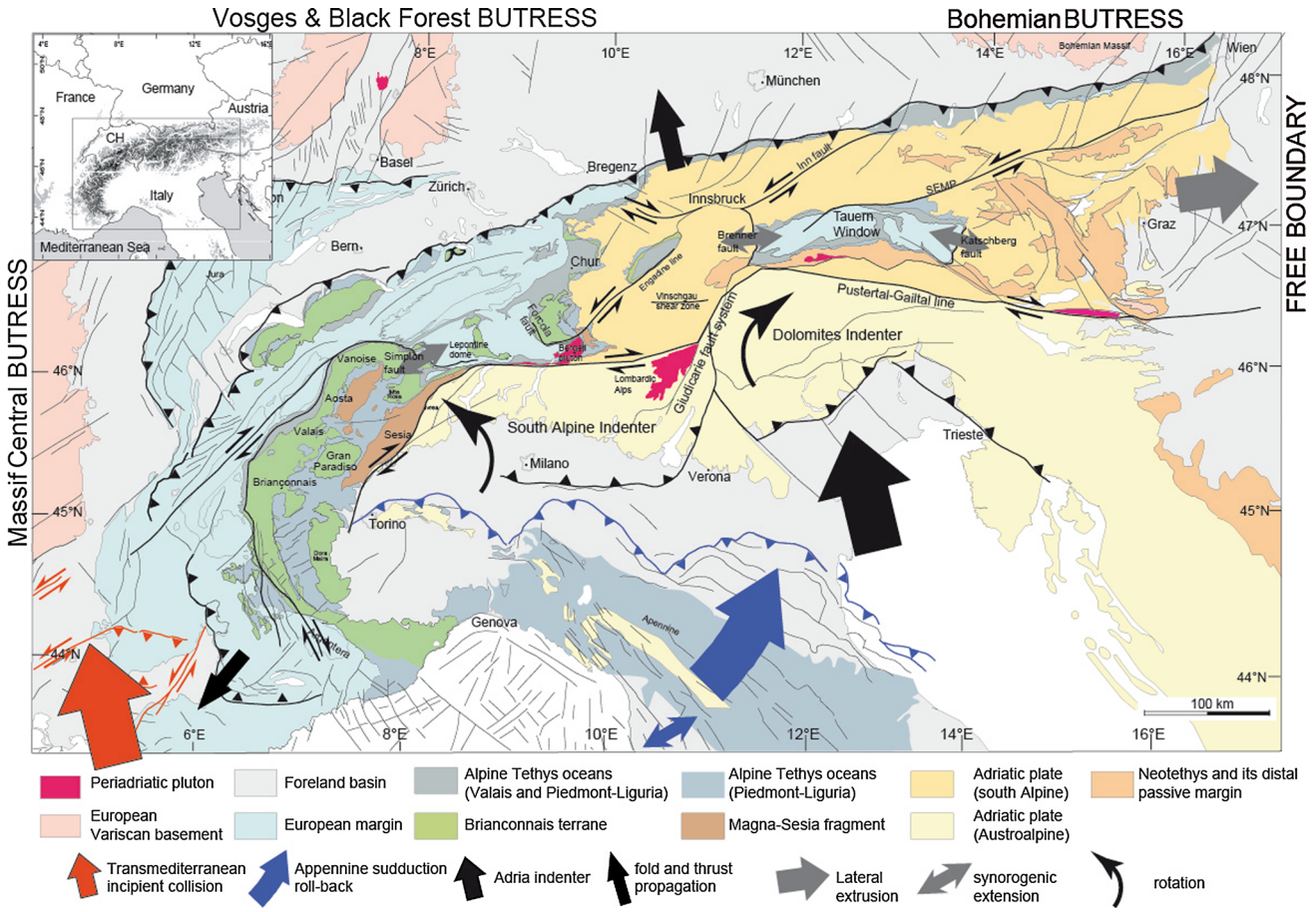

Fig. 1 Tectonic sketch map of the Alps within their geodynamic context (modified after Sue 1998; De Graciansky et al. 2011)

enhancing rapid rock uplift at the scale of the belt. Subsequent continental subduction induced complex vertical motions in the Alpine crust, which are still under debate both in terms of structures and dynamics (e.g. Champagnac et al. 2007; Sue et al. 2007; Vernant et al. 2013; Fox et al. 2015, 2016; Schlunegger and Kissling 2015; Zhao et al. 2015; Chéry et al. 2016; Nocquet et al. 2016). In the Eastern Alps, based on analogue models, extensional collapse and tectonic escape have been proposed as exhumation mechanisms during the Cenozoic (e.g. Ratschbacher et al. 1991, b).

Brittle deformations allow assessing the latest stage(s) of deformation of an orogen (e.g. Burg et al. 2005; Hintersberger et al. 2011). However, despite the large number of data on brittle deformation available over the entire European alpine chain (e.g. Sue and Tricart 1999, 2002, 2003; Sue et al. 1999, 2007; Bistacchi and Massironi, 2000; Champagnac et al. 2003, 2004, 2006; Ciancaleoni and Marquer 2008; Perrone et al. 2011; Beucher 2009; Allanic 2012; Bertrand et al. 2015) interpretation at the orogen scale has not been proposed in the Alps so far.

When comparing brittle deformations that occurred in different areas of the Alps, the timing of such deformation is of first importance. Because the closure temperature of fission-tracks in zircon crystals, i.e. 240 ± 60 °C (Yamada et al. 1995; Brandon et al. 1998), roughly corresponds to the brittle-ductile transition temperature in quartz in basement rocks (Stipp et al. 2002), at first approximation, the maximum age of brittle deformation can be inferred from the zircon fission-track ages. We are aware that using zircon fission-track age constraints for brittle deformation is a rough simplification that only allows for a large-scale overview over the entire alpine chain. Therefore, to provide a more accurate dating of the deformation we provide, when available, absolute dating of the deformations such as for the Central Alps (i.e. Zwingmann and Mancktelow 2004; Rolland et al. 2009; Allanic 2012), the Periadriatic fault system (Mancktelow et al. 2001; Müller et al. 2000, 2001; Martin et al. 2016), and the Southern Alps (Zanchetta et al. 2011).

In this work, we present a synthetic overview of brittle deformations in the Alps in order to reappraise the

significance of late-stage fracturing over the entire orogen in a wider geodynamic context by: (1) providing an overall homogeneous mapping of late Alpine brittle deformations, (2) using geochronological and thermochronological data to better constrain the timing of the brittle deformations, (3) analysing the degree of anisotropy of the upper mantle by questioning the significance of shear wave splitting from SKS phases.

2 Tectonic settings

The European Alps are geographically divided into the EW-trending Eastern Alps and the arcuate Western Alps (Fig. 1). They are characterized by a stack of large-scale nappes that are derived from Adria (Austroalpine nappes), the oceans of Alpine Tethys (part of the Penninic nappes) and Europe (Helvetic-Dauphinois cover nappes and Subhelvetic basements units) (e.g. Termier 1903; Argand 1916; Stampfli et al. 1998; Schmid et al. 2004). Stacking and exhumation of these nappes resulted from two successive orogenies that occurred from the Cretaceous onwards in the Eastern Alps and from the Cenozoic onwards in the Western Alps (Tollmann 1963; Frisch 1979; Platt 1986; Frank 1987; Behrmann 1988; Dewey et al. 1989; Froitzheim et al. 1996; Schmid and Kissling 2000).

In the Eastern Alps, subduction commenced during the Early Cretaceous and lasted until the Eocene (Handy et al. 2010). It is characterized by the subduction of continental crust associated with nappe stacking within the Austroalpine nappes in the Cretaceous and subsequent accretion of parts of the Tethyan oceanic units and finally European margin units to the Austroalpine in the Cenozoic (Schuster 2015 and reference therein). The underlying Penninic and Europe derived units formed an accretionary wedge in front of the Alpine subduction (e.g. Schmid and Kissling 2000; Weh and Froitzheim 2001). The following collisional orogeny took place from the Oligocene onwards (e.g., Dewey et al. 1973; Milnes 1978) and is related to the indentation of Adria into Europe (e.g. Tapponnier 1977; Sengör 1979; Schmid et al. 1996; Schmid and Kissling 2000; Handy et al. 2010; De Graciansky et al. 2011). The Eastern Alpine structures result from the northward movement of the Dolomites indenter with respect to the European plate, together with a coeval E–W extension favoured by the rifting of the Pannonian basin to the East (e.g. Ratschbacher et al. 1991a, b; Rosenberg et al. 2015) and eastward retreat of the subduction beneath the outer Carpathian belt (Decker et al. 1993; Royden 1993; Peresson and Decker 1997; Sperner et al. 2002). Related to this geodynamic context, the Eastern Alps, including the Southern Alps, display large-scale crustal strike-slip and extensional faults, i.e. the dextral Pustertal fault and Insubric line, the sinistral Salzach–Ennstal–Mariazell–Puchberg (SEMP) and Giudicarie fault systems and the Brenner and Katschberg normal fault systems (Fig. 1).

In the Western-Central Alps, orogeny took place from the Paleogene onward and is related to the gradual closure of the Tethyan oceans and the following Oligo-Miocene continental collision (Tapponnier 1977; Tricart 1984; Schmid and Kissling 2000; De Graciansky et al. 2011). They are characterized by voluminous occurrences of accreted rocks derived from the European plate (Fig. 1), i.e. the lowermost units of the Alpine chain, and additionally, accreted units derived from the Valais Ocean, the Briançonnais microcontinent and the Piedmont-Liguria oceans. All these units were accreted to the Adriatic margin (Southern Alps and Austroalpine nappes). The Western-Central Alps display an arc-shaped geometry, acquired during Oligocene time, due to complex rotation and deformations (Gidon 1974; Anderson and Jackson 1987; Vialon et al. 1989; Laubscher 1996; Thomas et al. 1999; Collombet et al. 2002; Delacou et al. 2005). The internal arc of the Western-Central Alps is imprinted by a series of Neogene to current extensional features related to extensional and/or transtensional processes. These processes are still under debate and could refer to two specific extensional phases (see Sue et al. 2007 for a review; Champagnac et al. 2007; Vernant et al. 2013; Walpersdorf et al. 2015; Nocquet et al. 2016).

South of the Pustertal-Gailtal fault, the Dolomites indenter forms a stack of basement and Upper Paleozoic to Mesozoic units (Laubscher 1985). South of the Insubric line, the Southern Alpine indenter displays the lower crust and the upper mantle of the Adriatic plate.

Hot and deep-rooted crustal material of the Eastern and Western-Central Alps has been exhumed asynchronously above the temperature for the brittle-ductile transition (ca. 300 °C). While the Eastern Alps, with the exception of the Tauern and the Engadine Windows, were already exhumed in Cretaceous times above c.a. 10 km, the Western-Central Alps were not exhumed above this depth before the Cenozoic (Fig. 2).

From the Oligocene to Miocene and Early Pliocene, the Western and Southern Alps expanded from the central axial zone, towards more external Europe and Adria, respectively, resulting from foreland propagation (Tricart 1984; Schmid et al. 1996; Schlunegger and Willett 1999; Willett et al. 2006). This was manifested by the widening of the area of rapid cooling towards more external parts of the orogen (Schlunegger and Willett 1999) and by the shift of the young orogenic activity (10–6 Ma) (Laubscher 1996) to the Jura Mountains and the external crystalline massifs to the West and to the Lombardian domain to the South-East (Fig. 2) (e.g. Laubscher 1996; Rabin et al. 2015).

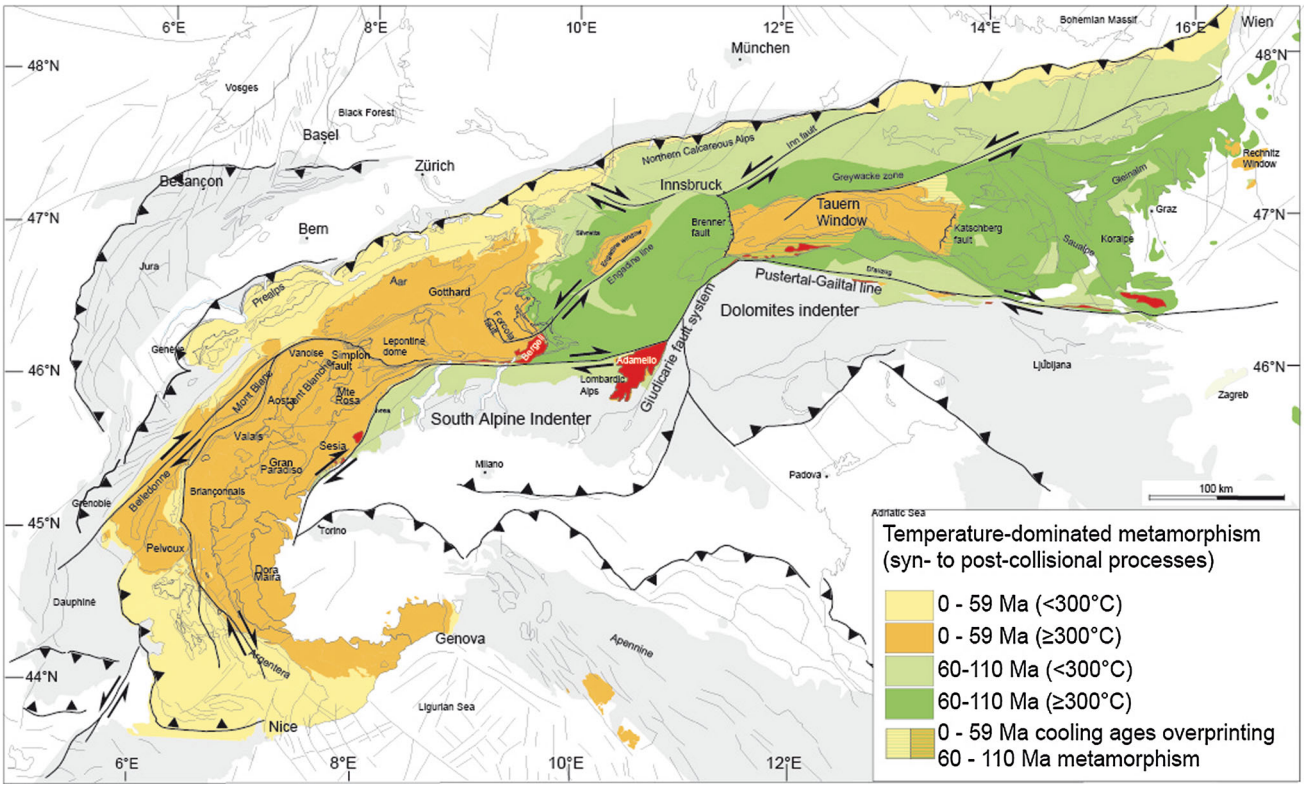

Fig. 2 Temperature dominated tectonometamorphic ages of the Alps (modified after Bousquet et al. 2004)

3 Overview of late-Alpine brittle deformation

3.1 Methodology

Systematic statistical analysis of brittle deformation measured in the field at meso/micro-scales allows quantifying the corresponding kinematic axes, either strain or stress axes, depending on the methodological and theoretical backgrounds (e.g. Wallace 1951; Bott 1959; Carey and Brunier 1974; Angelier and Mechler 1977; Angelier and Goguel 1979; Angelier 1989; Gephart 1990; Twiss and Unruh 1998; Yamaji 2000). Regardless of whether a stress or kinematic approach is taken, slip occurs parallel to the direction of maximum resolved shear stress within the fault plane that is subject to a local spatially homogeneous stress tensor leading to failure (Wallace 1951 and Bott 1959's principle). The basic assumptions for the application of methods of stress/strain analysis of brittle deformation are the following: (1) the rock volume is isotropic and homogeneous; (2) displacements along faults are incremental and individual faults slip independently; (3) the stress/strain field is uniform and steady during a given tectonic phase; (4) the deformation is non-rotational; (5) no post-faulting reorientation of the fault-slip data has occurred. In practice, the direction of movement is mainly given by the orientation of slickensides, mineral fibres, and grooves on the fault plane. The sense of movement is given, among other indicators, by steps, Riedel criteria (Riedel 1929), fibres and drag-folds (e.g. Petit 1987). Although the related methods have proved their robustness in many areas and in various tectonic contexts (e.g. Burg et al. 2005; Hintersberger et al. 2011), fault-slip data may not be in accordance with these basic assumptions, mainly because of stress variations due to pre-existing anisotropies and inherent rock heterogeneities. The long-lasting discussions on the various methods concerning strain vs. stress approaches have recently been critically discussed (Lacombe 2012), and we refer to this paper and references therein for more details.

Brittle deformations of the entire Alps have been investigated by different authors and paleostress fields have been determined using the graphical right-dihedra method (Angelier and Mechler 1977; Pfiffner and Burkhard 1987), the graphical P-B-T axes method (Turner 1953; Marrett and Allmendinger 1990), as well as the numerical standard direct inversion (Angelier 1990; Sperner et al. 1993). In particular, the direct inversion method [see Angelier (1990) for the theoretical formalism] defines a stress tensor that best minimizes the deviation between the theoretical shear stress for a given plane and slickenside, and the measured slickenside lineation (Carey and Brunier 1974; Angelier 1989, 1990).

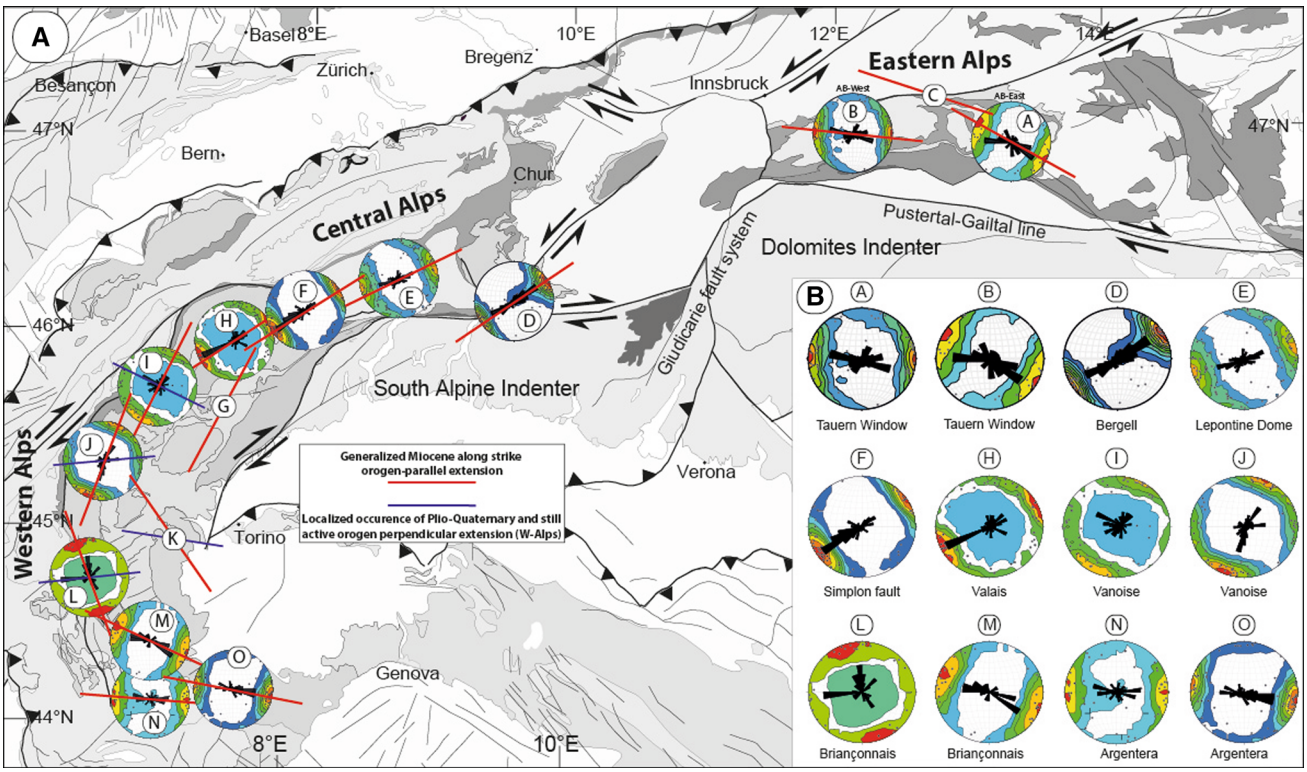

Fig. 3 **a** Synthetic map of the regional best σ3 axes determined from the statistical analysis of paleostress databases available around the bend of the Alps (see text for details). The stereonets (or only the best axes in red drawn from the corresponding publication for the localities **c**, **g**, **k**, where numerical datasets are unavailable) correspond to the Tauern Window (**a**, **b**; Bertrand et al. 2015; and **c** Wang & Neubauer 1998), the Bergell pluton (**d**; Ciancaleoni and Marquer 2008), the Lepontine Dome (**e**; Allanic 2012), the vicinity of the Simplon fault (**f**: Grosjean et al. 2004), the Valais area (**h**; Champagnac et al. 2003), the Aosta area (**i**; Champagnac et al. 2004; **g**; Bistacchi and Massironi 2000), the Vanoise area (**j**; Champagnac et al. 2006), The Cotian Alps (**k**; Perrone et al. 2011), the Briançon area between the Pelvoux, Viso and Argentera massifs (**l**, **m**; Sue and Tricart 1999; 2002; 2003 and **n** Bauve et al. 2014), and the Penninic units north of the Argentera massif (**o**; Beucher 2009). In red, σ3 for the major orogen-parallel extension signal; in blue, σ3 for the minor orogen-perpendicular extension signal recognized in the core of the Western Alpine arc (see text for details). See Fig. 1 for geological caption. **b** Set of statistical stereonets for each of the dataset plotted in **a**. Each stereonet presents the contouring of the overall related paleostress σ3 axes, together with the corresponding rose-diagram (Stereonet© software, Allmendinger et al. 2013; Cardozo and Allmendinger 2013). Due to their internal regional variability, the datasets of the Tauern Window, Valais-Vanoise and the Briançonnais areas have been subdivided into 2 or 3 regional stereonets. The corresponding parameters are given in Table 1, including the best σ3 directions in the (0°–180°) range (Bingham axial distribution, see Allmendinger et al. 2013 Cardozo and Allmendinger 2013). The overall paleostress/strain database (727 tensors) is available as supplementary material together with the corresponding maps

3.2 Data compilation

We present hereafter a synthesis of data on brittle deformation over the entire Alpine belt, especially along the axial zone of the Alps. We integrated available datasets (Fig. 3a, b) from the Penninic units north of the Argentera massif (Beucher 2009; Bauve et al. 2014), the Briançon region between the Pelvoux, Viso and Argentera massifs (Sue and Tricart 1999, 2002, 2003), the Vanoise area (Champagnac et al. 2006), the Aosta region (Champagnac et al. 2004; Bistacchi and Massironi 2000), the Valais area (Champagnac et al. 2003), the vicinity of the Simplon fault (Grosjean et al. 2004), the Lepontine Dome (Allanic 2012), the Bergell pluton (Ciancaleoni and Marquer 2008), the Tauern Window (Bertrand et al. 2015), along the SEMP (Salzach–Ennstal–Mariazell–Puchberg; Wang and Neubauer 1998), along the Passeier and Jaufen faults (Luth 2011) and in the Cottian Alps (Perrone et al. 2011).

To summarize the paleostress field(s) around the bend of the Alps, we reassessed a homogeneous statistical analysis for the entire set of data (Fig. 3a, b; Table 1). The reading of the 727 tensors map being quite difficult (see supplementary material), we propose a new statistical map-view (Fig. 3a) that includes both contouring of stereonets and rose-diagrams for each regional subset of data. The results are plotted on Fig. 3b. Each stereonet in Fig. 3 presents both the contouring of the overall related σ3 paleostress axes for a given area, together with the corresponding rose-diagram (Stereonet© software, Allmendinger et al. 2013; Cardozo and Allmendinger 2013). The corresponding parameters are given in Table 1, including the best σ3 directions in the (0°–180°) range (Bingham axial

Table 1 Statistical parameters of the average σ3 for each sub-dataset analysed (see text for details)

CODE (see Fig. 3)	References	N-data	Specific localization	Average dominant s3 dir. [0–180] (°)	* Secondary s3 dir. [0–180] (°)
A	Bertrand et al. (2015)	30	lon > 12.5°	119	
B	Bertrand et al. (2015)	68	lon < 12.5°	95	
C	Wang and Neubauer (1998)	–	See ref. D3 D4 phases	105	
D	Ciancaleoni & Marquer (2008)	111	See ref.	56	
E	Allanic (2012)	105	See ref.	64	
F	Grosjean et al. (2004)	60	See ref.	58	
D	Bistacchi and Massironi (2000)	–	See ref. D2 phase	60	
H	Champagnac et al. (2006)	90	lat > 46°	63	
I	Champagnac et al. (2006)	58	45.5° < lat < 46	27	116
J	Champagnac et al. (2006)	68	lat < 45.5°	21	85
E	Perrone et al. (2011)	–	See ref.	145	95
L	Sue and Tricart (2003)	28	lat > 44.75°	160	84
M	Sue and Tricart (2003)	30	lat < 44.75°	115	
N	Bauve et al. (2014)	46	See ref.	94	
O	Beucher (2009)	79	See ref.	101	

CODE refers to the name of each sub-dataset; reference gives the corresponding publication with the complete description of the data and stress inversion methodologies; N-data is the number of paleostress tensors included in the statistical handling; specific localization provides the limits of the boxes used for the subdividing of the datasets of the Tauern Window, the Valais, Aosta, Vanoise and Briançonnais areas; average dominant σ3 is the σaverage σ3 direction for each dataset, regarding both the contouring and best-axis computing and the rose diagram distribution, given in the (0°–180°) range; secondary σ3 is the direction of the secondary extensional signal (orogen-perpendicular, still active), given in the (0°–180°) range only where it is significant enough

*significant occurrence of orogen perpendicular secondary extension (see discussion in Sue et al. 2007)

distribution combined with the rose-diagram distribution). From the south-western branch of the chain to the core of the Eastern Alps, the paleostress field displays a dominant and surprisingly stable signal that displays horizontal to subhorizontal σ3 paleostress axes running parallel to the orogen along the bending of the belt (highlighted by the red lines in Fig. 3a). Note that the stereonets of the Briançonnais (L), the Valais (I), The Cottian Alps (K), and the Western-Aosta (J) areas present a noticeable secondary family of horizontal σ3 oriented perpendicular to the Western Alpine arc (Sue and Tricart 2002; Champagnac et al. 2006; Perrone et al. 2011). Kinematically, orogen-parallel horizontal extension by normal faulting is often associated with horizontal extension by strike-slip faulting (Champagnac et al. 2006; Sue et al. 2007; Beucher 2009; Bauve et al. 2014). In the overall belt, ca. 75% of the computed paleostress tensors are normal fault tensors, while most of the remaining ones are transcurrent. Over the entire inner Alps, orogen-parallel normal fault and strike-slip tensors are kinematically coherent, that is to say the σ_3 paleostress axes remain subparallel and near-horizontal regardless of the type of tensor (Wang and Neubauer 1998; Sue and Tricart 1999, 2002, 2003; Bistacchi and Massironi 2000; Champagnac et al. 2003, 2004; Grosjean et al. 2004; Champagnac et al. 2006; Ciancaleoni and Marquer 2008; Beucher 2009; Luth 2011; Perrone et al. 2011; Allanic 2012; Bauve et al. 2014; Bertrand et al. 2015).

The major orogen-parallel extensional signal is very stable over the entire Alps and follows the arcuate shape of the belt, especially in the Western Alps' arc (Fig. 3a). In detail, the so-called Central Alps northeast of the Western Alpine arc including the Valais (Champagnac et al. 2003), Simplon area (Grosjean et al. 2004), Lepontine Dome (Allanic 2012), Bergell pluton (Ciancaleoni and Marquer 2008) display an overwhelming majority of orogen-parallel σ_3 paleostress axis tensors within a very regular ENE-WSW σ_3 orientation (average N60°, Fig. 3a over more than 250 km along the strike of the orogen. Further east, the Tauern Window shows a quite comparable orientations of σ3 (WNW-ESE, N105° on average) (Bertrand et al. 2015), with a variation from the Western Tauern Window (N95°) to the Eastern Tauern Window (N119°). Southward, from the Vanoise area to the Briançon region and the internal units North of the Argentera, late Alpine extension perfectly follows the arcuate shape of the orogenic arc, with σ_3 axes evolving from N27° in the North of the arc, to N160°, N105°, then N101° in the southernmost branch of the arc (Table 1; Fig. 3a).

Orogen parallel extension, reflected by the σ_3 paleostress axes, has long been described in the Eastern Alps (Behrmann 1988; Selverstone 1988; Ratschbacher et al. 1989) and in the Central Alps (Steck 1980; Mancktelow 1985), mainly based on the analysis of ductile deformation, but it was only later recognized in the Western Alps on the

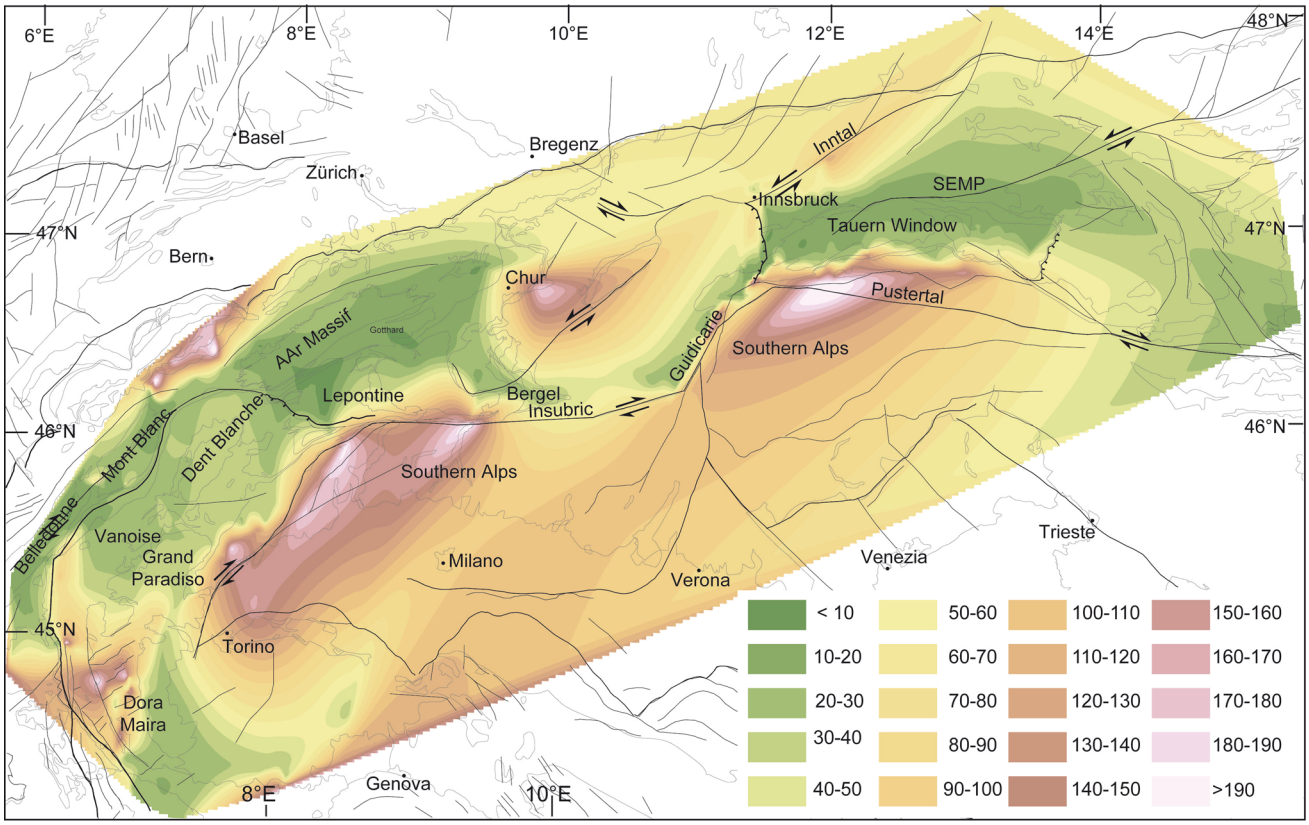

Fig. 4 Interpolation of zircon fission-track ages over the Alps. Interpolation is made using the natural neighbour tool of ArcGis ® software and 492 zircon fission-track ages compiled based on the following published data: Carpena and Caby 1984; Hurford and Hunziker 1985, 1989; Carpena et al. 1986; Flisch 1986; Bürgi and Klötzli 1990; Michalski and Soom 1990; Soom 1990; Hejl and Wagner 1991; Stöckhert 1991; Carpena 1992; Seward and Mancktelow 1994; Fügenschuh 1995; Fügenschuh et al. 1997, 1999; Elias 1998; Sachsenhofer et al. 1997; Bertotti et al. 1999; Seward et al. 1999; Schwartz 2000; Mancktelow et al. 2001; Viola et al. 2001; Bigot-Cormier 2002; Steenken et al. 2002; Ceriani et al. 2003; Dunkl et al. 2003; Fügenschuh and Schmid 2003; Most 2003; Keller et al. 2005; Wölfler et al. 2008; Pomella et al. 2011, 2012; Bertrand et al. 2017

basis of the analysis of brittle structures (see Champagnac et al. 2006 for a review). In this framework, our synthesis of fault-related data over the entire Alpine belt shows a surprisingly steady signal with a very dominant paleostress field characterized by σ_3 paleostress axes distributed parallel to the strike of the belt, from its eastern tip, to its southwestern end. Our synthesis establishes a tectonic continuity regarding this orogen-parallel extension over the entire Alpine chain.

4 Age of the brittle deformations

4.1 Upper limit

The closure temperature of fission-tracks in zircon crystals is estimated around 240 ± 60 °C (Yamada et al. 1995; Brandon et al. 1998). The annealing kinetics of fission-tracks in zircon, and therefore the closure temperature, depends on different parameters such as the chemical composition of the minerals, the presence of radiation-damages in the crystal (Dodson 1973; Kasuya and Naeser 1988; Garver et al. 2005) or the cooling rates. However, as a first approximation, we assume that the closure temperature of fission-tracks in zircon corresponds roughly to the temperature of the brittle-ductile transition in quartz in basement rocks (i.e. 280 ± 30 °C; Stipp et al. 2002).

We provide an interpolated map of a compilation of non-detrital zircon fission-track ages over the entire Alps using the natural-neighbour algorithm tool of ESRI-ArcMap10^{tm} GIS software (Fig. 4). Extended cells for the interpolation are of 500 m. Analytical errors are not taken into account for the interpolation. Age classes are based on the analysis of the distribution histograms of zircon fission-track ages. Because of the history of detrital materials (e.g. Cerveny et al. 1988; Brandon and Vance 1992), it is difficult to assess the significance of the fission-track ages in such material; therefore detrital fission-track ages are here not considered.

The Argentera, Dora-Maira, Grand Paradiso, Belledonne, Mont-Blanc massifs of the Western Alps, the Lepontine Dome and the Bergell pluton in the Central Alps, and the Tauern Window, as well as units located northwest of the Meran-Mauls fault and southeast of the Jaufen fault cooled below the zircon fission-track closure temperature during Late Paleogene and Neogene. The rest of the Alps and especially the Austroalpine units of the eastern Alps cooled below this temperature between Jurassic and Eocene (Fig. 4). Therefore, the main areas of interest in this paper are the area around Briançonnais, the Valais-Vanoise area, the area around the Simplon fault, the Lepontine Dome, the Bergell pluton and the Tauern Window. With the exception of the Briançonnais, all the investigated areas display zircon fission-track ages of Oligocene and younger age. As stated previously, the zircon fission-track closure temperature corresponds to the ductile–brittle transition temperature, therefore deformations measured in those areas are of Miocene or younger age.

The Bergell area is a good target for investigating brittle deformations because of the homogeneous rheological behaviour of the granitoids and of its Oligocene emplacement (32–30 Ma) (Von Blanckenburg et al. 1992), which provides a good constrain on the maximum age of the deformations. Moreover, the Bergell area displays close relationships between well-constrained time markers of post-collisional deformation (late Oligocene Periadriatic intrusions) and prominent late Alpine faults of the Periadriatic fault system (Tonale, Engadine and Forcola faults). After emplacement of the Bergell pluton, uplift and eastward escape of the area occurred between the dextral Tonale fault and the sinistral Engadine fault as the result of on-going N–S shortening (Schmid and Froitzheim 1993). A late Oligocene-early Miocene zircon fission-track age (23.1 ± 1.4 Ma; Ciancaleoni 2005) provides a good constraint on the timing of cooling below the ductile–brittle transition temperature for the Bergell pluton.

To the south, the dense fault network, which carves the Briançonnais zone, postdates all the Alpine Oligocene-age (Tricart 1984) compression-related structures such as nappe stacking, folds, schistosities and cleavages related to the different compressional phases (Sue and Tricart 1999, 2003). Therefore, it is has been proposed that the brittle deformations in the Briançonnais area correspond to the last tectonic event in the Alpine history, potentially of Miocene age (Sue and Tricart 2003). Local paleo-karst infill allowed proposing that brittle deformations corresponding to the last orogen-perpendicular and still active extension worked during the Pliocene using indirect argumentation (Sue 1998), In summary, in the Briançon and surrounding areas, the orogen-parallel extension phase is most likely of Miocene age, postdating the Oligocene compressional phases, and followed by the Plio-Quaternary and still active orogen-perpendicular extension.

4.2 Dating of faults

Direct dating of brittle faulting is generally difficult and hence rare. Only a few methods allow such a direct dating such as the dating of pseudotachylite that develop during seismic events by extreme grain size reduction and melting due to frictional heating (e.g. Spray 1992; Hetzel et al. 1996). If the pseudotachylites contain significant amounts of potassium derived from the host rock minerals, they may be suitable to assess the timing of fault activity by using the $^{39}Ar/^{40}Ar$ method (e.g., McDougall and Harrison 1999; Van der Pluijm et al. 2001). Displacement on brittle fault planes may also often result in the development of fault gouge, composed of crushed rock fragments and authigenic clay minerals formed by retrograde hydration reactions. Dating the activity of such brittle faulting is thus possible by using K–Ar on those authigenic clay minerals (Lyons and Snellenberg 1971; Kralik et al. 1987).

In the Alps, data based on such methods are rare, and specifically located within the Lepontine Dome (Allanic 2012), in the vicinity of the Periadriatic fault system (Mancktelow et al. 2001; Müller et al. 2000, 2001; Zwingmann & Mancktelow 2004) and in the Aar massif (Rolland et al. 2009) (Fig. 5).

Absolute dating based on K–Ar ages of fault gouges provides ages of 6.01 ± 0.18–7.17 ± 0,18 Ma along the N–S striking latest and brittle part of the Simplon detachment, and 8.72 ± 0.26 Ma along the EW-striking Centovalli fault (Zwingmann and Mancktelow 2004). These ages are coherent with absolute ages based on $^{40}Ar/^{39}Ar$ dating of pseudotachylites of the Simplon detachment and within the Lepontine Dome area (between 7.7 ± 0.01 and 11 ± 2 Ma, Allanic (2012) (Fig. 5). Moreover, $^{40}Ar/^{39}Ar$ and Rb/Sr dating of synkinematic white mica of in foliated phyllonites from the footwall of the Simplon detachment yields ages between 14.6 ± 9.5 and 11.0 ± 0.1 Ma (Campani et al. 2010), and are interpreted to estimate the timing of the ductile–brittle transition. Based on these ages, it has been proposed that the Simplon low angle detachment underwent a continuous transition from ductile shearing to brittle deformation within the same geological framework from Middle Miocene time onwards (Campani et al. 2010). K–Ar for <2 μm illite fractions fault gouges provide ages of 18.98 ± 0.47–23.46 ± 047 for the steeply north-dipping Insubric fault south of the Lepontine Dome, and 15.89 ± 0.33 Ma for the Pustertal-Gailtal fault at the tip of the South Alpine indenter (Zwingmann and Mancktelow 2004). Stepwise-heating and laser-ablation $^{40}Ar/^{40}Ar$ of pseudotachylites and Rb–Sr on mylonites of

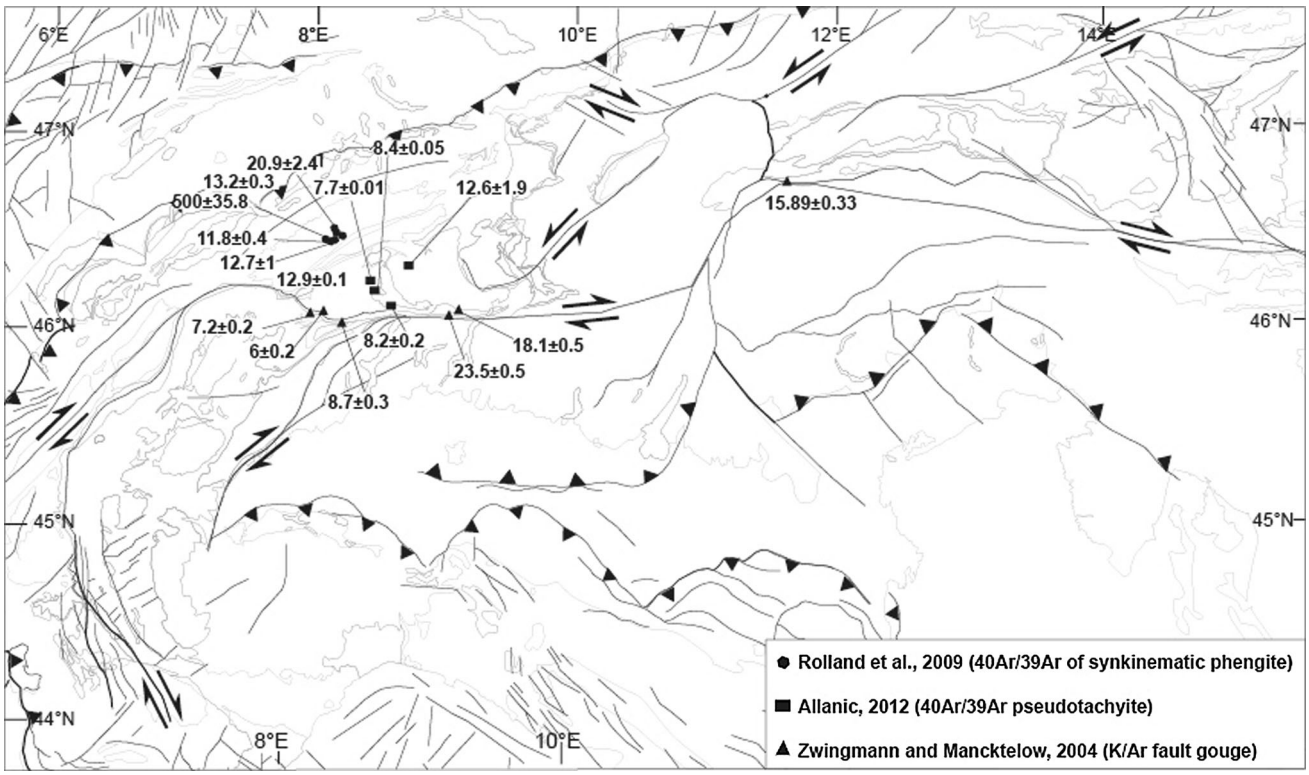

Fig. 5 Dating of brittle faulting based on the K–Ar method on authigenic clay minerals and $^{39}Ar/^{40}Ar$ dating of pseudotachylites in the Alps (modified after Zwingmann and Mancktelow 2004; Ciancaleoni 2005; Rolland et al. 2009; Allanic 2012)

the Periadriatic fault system indicate a tectonic activity lasting from Late Cretaceous to Middle Miocene (Müller et al. 2000, 2001; Mancktelow et al. 2001). In the Aar massif, brittle–ductile offsets and reactivation of shear zones are constrained between 13.8 ± 0.2 Ma and 12.2 ± 0.2 Ma ($^{40}Ar/^{39}Ar$ on syn-kinematic phengite, Rolland et al. (2009), while brittle deformations are dated between 10.1 ± 0.4 Ma and 7.6 ± 0.4 Ma (K–Ar on mylonite and fault gouges clays, Kralik et al. (1992). Most of the above-mentioned age data are related to brittle deformation belonging to the orogen-parallel extensional phase (Fig. 5, Zwingmann and Mancktelow 2004; Allanic 2012), and are coherent with the zircon fission-track ages (Fig. 4). Absolute dating combined with zircon fission-track dating suggests that such orogen-parallel extension occurred during late Oligocene to Miocene times.

5 Discussion

Crustal thickening due to on-going orogen-perpendicular convergence accommodates large amounts of intra-continental shortening across the Alpine belt during late-stage indentation of Adria. However, brittle deformations in the Western, Central and Eastern Alps display surprisingly similar patterns with major occurrence of brittle faulting achieving subhorizontal extension parallel to the strike of the Alpine chain. This Neogene orogen-parallel extensional signal developed mainly in the internal zones, coevally with further propagation of the indentation to the West and the Northwest in the external zone. Indeed, the propagation of the Alpine front in the Western Alps and the northward movement of the Southern Alpine and Dolomites indenters in the Central and Eastern Alps and backthrusting onto the Adria microplate were accommodated by orogen-parallel extension in the inner zones, at the scale of the entire chain. This implies major tectonic decoupling between the inner belts and the most external belts of the Alps as a whole. Late Alpine orogen-parallel extension appears as a major event during the kinematics and associated dynamics of the evolution of the Alps from the Miocene onwards. It can no longer be treated as a local epiphenomenon, and must therefore be taken into account in geodynamic models for the Miocene geodynamic evolution of the Alps.

In the Lepontine Dome and the Bergell pluton, most of the collisional shortening due to the north-directed component of the movement of the South Alpine indenter was accommodated by the formation of large-scale upright folds. In the Eastern-Alps, the late brittle deformations, as observed in the Tauern Window are dominated by orogen-parallel extension at the eastern and western borders of the Dome and by strike-slip faulting in the central parts of the

Dome and along the SEMP (Fig. 3) (Wang and Neubauer 1998; Bertrand et al. 2015). The location of the Tauern Window in front of the tip of the Dolomites indenter invokes a possible link of extensional and strike-slip faulting with the N to NNE motion of the Dolomites indenter. Analogue models (Ratschbacher et al. 1991a, b; Rosenberg et al. 2004, 2007) show that the movement of the indenter can be accommodated, in the eastern Alpine units located north of the indenter, by both extension and shortening due to deformation partitioning. Northward movement of the indenter first resulted in exhumation of the unit of the lower European plate and the overlying Penninic units of the Tauern Window by folding and erosion accommodating ca. 30 km of orogen-perpendicular N–S shortening of the Tauern window (Scharf et al. 2013). During the Neogene, the motion of the Dolomites indenter was accommodated by orogen-parallel extension combined with strike-slip faulting, yielding an overall N–S shortening and exhumation of ca.10 km (Bertrand et al. 2015). Orogen-parallel extension in the Eastern Alps is inferred to be driven either by the retreat of the plate boundary in the outer Carpathians (Royden 1993; Sperner et al. 2002) or by a combination of N–S compression driven by the Dolomites indenter (Ratschbacher et al. 1991a) and eastward retreat of the subducted slab below the Carpathians (Decker et al. 1993; Peresson and Decker 1997). Mid- to Late Miocene (U-Th–Sm)/he and apatite fission-track ages from the Southern Alps and the Karawanken Mountains (Nemes 1996; Zattin et al. 2003, 2006; Pomella et al. 2011; Reverman et al. 2012; Heberer et al. 2016), indicate that exhumation related to the movement of the Dolomites indenter, which was localized within the central part of the Eastern Alps during Oligocene and Early Miocene became more widespread during Mid- to Late Miocene (Heberer et al. 2016).

Images of the seismic velocity and anisotropy variations in the uppermost mantle, compiled from Pn and Sn phases (Diaz et al. 2013) indicate a non-continuous signature of the Alps, with an arcuate variation of the anisotropic properties in the Western Alps and low-velocity zones beneath its eastern and southwestern terminations. *Pn* anisotropy shows consistent orientations subparallel to major alpine orogenic structures. Beneath the Alps, the two important low velocities observed seem to be separated by a zone of normal velocity located roughly under the Insubric line. The anisotropic parameters obtained from *Pn* and *SKS* splitting are very similar beneath the Western Alps, with an anisotropy following the trend of the belt, from a NE–SW orientation to the North, to a roughly NS orientation in the southern termination of the Alps. The variations in crustal thickness are consistent with available Moho depths inferred from controlled-source seismology and receiver functions (Spada et al. 2013). The overall similarity between anisotropic parameters retrieved from *Pn* tomography (Diaz et al. 2013), from the splitting *SKS* (Qorbani et al. 2015a) and the Moho depth (Spada et al. 2013) seems to indicate that deformations are rather uniform from the base of the crust to mantle depths. The anisotropic pattern may be explained by lithospheric-scale deformation beneath the Alps triggered by mantle flow that may be related to the retreat of the Pannonian and Calabrian slabs (Faccenna et al. 2014) at both ends of the Alpine orogen.

SKS splitting measurements also indicate a strong coherent average signal with the fast direction being subparallel to the strike of the orogen over the entire Alps, including Central and Western Alps (Qorbani et al. 2015). It is SW–NE in the western part of the Eastern Alps and NW–SE in the eastern part of the Eastern Alps and turns parallel with the arcuate shape of the Central-Western Alps (Fig. 6), staying roughly parallel to the strike of the belt. In Fig. 6, we superpose the orientations of the inferred axes of subhorizontal orogeny-parallel extension from our statistical analysis with the orientations of the fast direction inferred from SKS measurements. In this framework, it appears that both kinds of data, a priori disconnected as belonging to very different structural levels within the lithosphere, exhibit surprisingly similar patterns. Indeed, the scheme of the SKS anisotropy, arising from lattice preferred orientation of olivine acquired during upper mantle flow parallel to the fast direction, is well correlated with the orientation of the extensional axes measured in the upper crust along the entire strike of the Alps. This might indicate a coupling between strain in the upper crust (acquired during brittle deformation) and flow in the upper mantle (acquired during dislocation creep in olivine at very elevated temperatures of >700 °C). Beyond the discussion on a potential fortuitous correlation, we can propose that, at the scale the entire Alps, Miocene upper crustal brittle deformation, characterized by an orogen-parallel extensional phase, could be controlled, or at least strongly influenced, by mantle flow (e.g. Doglioni 1991; Faccenna et al. 2004; Jolivet et al. 2008; Molli et al. 2010). Such a provocative interpretation would imply a strong coupling across the different structural levels in the Alpine lithospheric root.

The main features of brittle deformation in the Eastern Alps are related to lateral extrusion resulting from the northward movement of the Dolomites indenter combined with slab retreat beneath the Carpathians. However, in the Western Alps the overall structure of the arc prevents to propose a similar extrusion-like model. Here, deformations and exhumation are related to the WNW-directed movement and counterclockwise rotation (e.g. Delacou et al. 2005 and references herein) of the South Alpine indenter in the Oligocene and Miocene times (e.g. Tricart 1984;

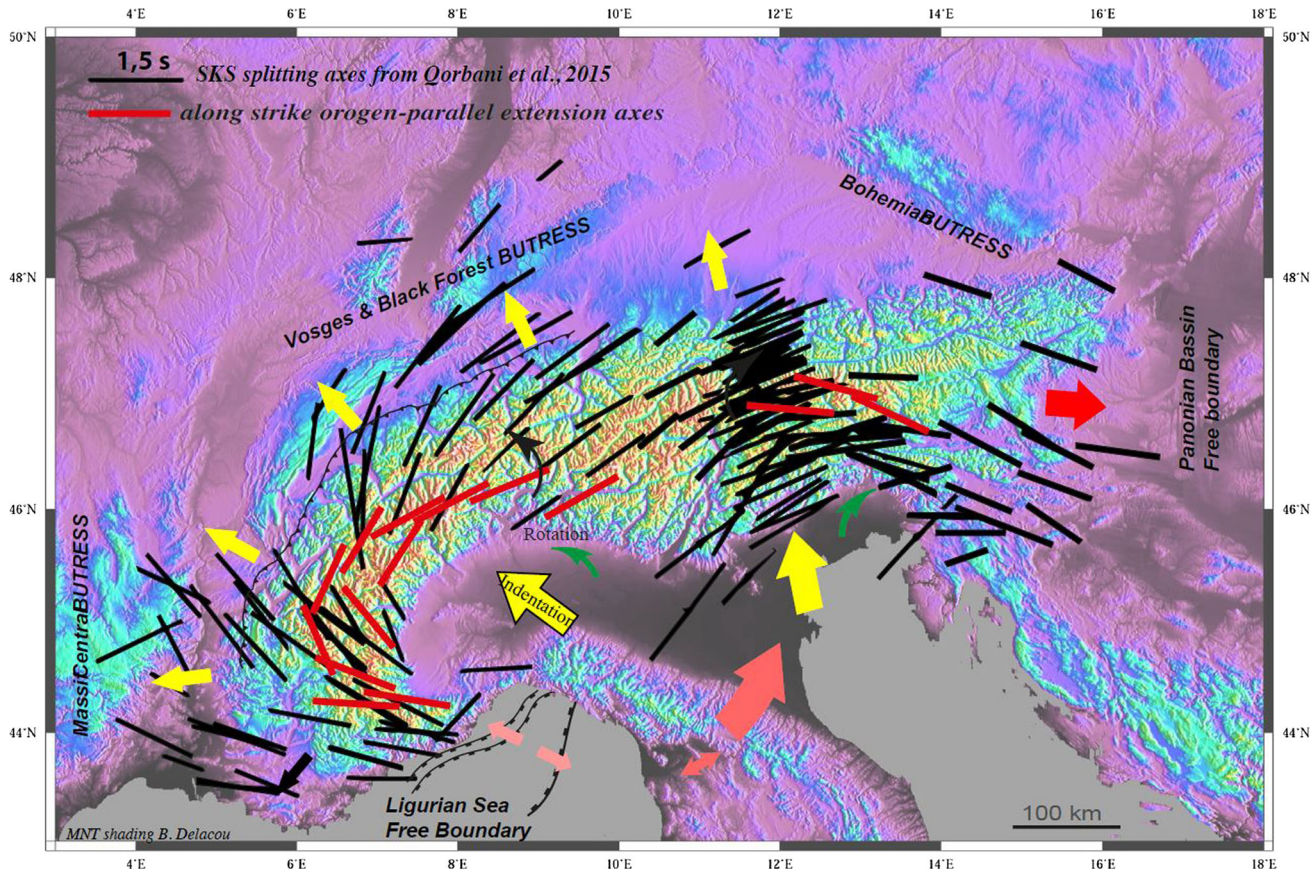

Fig. 6 Map of average SKS (*black lines*) (modified after Qorbani et al. 2015b) and extension direction *(red arrows*: orogen-parallel extension; *blue arrows*: orogen-perpendicular extension) showing the correlation between these two sets of data. The overall Neogene geodynamic state of the Alps is plotted with coloured *large arrows* around the bend of the belt, including propagation of thrusting in the outer zones, North and West of the orogen, rotations of the Adriatic indenter, and opening of the Ligurian sea (see Sue et al. 2007 for further details)

Schmid and Kissling 2000; Schmid et al. 2017). The opening of the Ligurian Sea during Early-Middle Miocene may have favoured the brittle extension parallel in an overall geodynamic model, in which orogen-parallel Miocene extension in the upper crust of the internal Alps would be driven by mantle flow and concomitant slab retreat processes implying the Pannonian slab to the East and the Apennine slab to the Southwest.

6 Conclusion

We provided a first synthesis of the late Alpine brittle deformation at the scale of the entire Alps, using inversion methods and published regional paleostress fields (Sue and Tricart 1999, 2002, 2003; Champagnac et al. 2003, 2004, 2006; Grosjean et al. 2004; Ciancaleoni and Marquer 2008; Beucher 2009; Allanic 2012; Bertrand et al. 2015). 727 individual tensors have been statistically reassessed to provide an overview of the main kinematics associated to the late faulting in the Alps. Zircon fission-track ages, direct dating, and indirect argumentations suggest that the main faulting event is a Miocene phase of orogen-parallel extension, well developed in the inner belts of the entire Alps, from the Eastern Alps (E–W extension) to the Central Alps (ENE–WSW extension) and the Western Alpine arc (rotation of the extensional axes from NE-SW to NW–SE). Indeed, orogen-parallel extension is surprisingly stable along the strike of the Alps. Correlation between brittle extension axes and SKS anisotropy axes along the strike of the Alps suggest a potential coupling between mantle flow within the upper mantle and the upper crustal faulting. In this framework, Miocene orogen-parallel upper crustal faulting would be driven (at least partly) by mantle flow, which itself is controlled by subduction dynamics in the larger Alpine-Mediterranean realm.

Acknowledgements This work was supported by the Budapest and Besançon Universities, the French CNRS, and the OSU-THETA (Besançon observatory). We wish to thank C. Allanic and R. Beucher for making their data available in their PhD. Many thanks to the colleagues we met at the 12th Alpine Workshop for fruitful discussion. We greatly thank H. Pomella, C. Faccenna, and a third

anonymous reviewer, as well as the editor S. Schmid for their constructive comments.

References

Allanic, C. (2012). *Kinematics, Age and Dynamic of the Brittle Deformation within the Lepontine Dome (Central Alps)*. Ph.D. dissertation, University of Orléans, Orléans, France, 272 pp.

Allmendinger, R. W., Cardozo, N. C., & Fisher, D. (2013). *Structural geology algorithms: vectors and tensors* (p. 289). Cambridge: Cambridge University Press.

Anderson, H., & Jackson, J. (1987). Active tectonics in the Adriatic region. *Geophysical Journal International, 91,* 937–983.

Angelier, J. (1989). From orientation to magnitudes in paleostress determinations using fault slip data. *Journal of Structural Geology, 11,* 37–50.

Angelier, J. (1990). Inversion of field data in fault tectonics to obtain the regional stress – III. A new rapid direct inversion method by analytical means. *Geophysical Journal International, 103,* 363–376.

Angelier, J., & Goguel, J. (1979). Sur une méthode simple de détermination des axes principaux des contraintes pour une population de failles. *Comptes Rendus de l'Académie des Sciences, 282,* 307–310.

Angelier, J., & Mechler, P. (1977). Sur une méthode graphique de recherche des contraintes principales également utilisable en tectonique et séismologie: la méthode des dièdres droits. *Bulletin de la Société Géologique de France, 7,* 1309–1318.

Argand, E. (1916). Sur l'arc des Alpes occidentales. *Eclogae Geologicae Helveticae, 14,* 145–191.

Argand, E. (1924). La tectonique de l'Asie. *Compte-rendu du XIIIème Congrès Géologique International, 1922*(1), 171–372.

Bauve, V., Plateaux, R., Rolland, Y., Sanchez, G., Bethoux, N., Delouis, B., & Darnault, R. (2014). Long-lasting transcurrent tectonics in SW Alps evidenced by Neogene to present-day stress fields. *Tectonophysics, 621*, 85–100. doi:10.1016/j.tecto.2014.02.006.

Behrmann, J. H. (1988). Crustal-scale extension in a convergent orogen: the Sterzing-Steinach mylonite zone in the Eastern Alps. *Geodynamica Acta, 2,* 63–73.

Bertotti, G., Seward, D., Wijbrans, J., Ter Voorde, M., & Hurford, A. J. (1999). Crustal thermal regime prior to, during, and after rifting: a geochronological and modeling study of the Mesozoic South Alpine rifted margin. *Tectonics, 18,* 185–200.

Bertrand, A., Rosenberg, C. L., & Garcia, S. (2015). Fault-slip analysis and late exhumation of the Penninic units of the Tauern Window, Eastern Alps. *Tectonophysics, 649,* 1–17.

Bertrand, A., Rosenberg, C. L., Rabaute, A., Herman, F., & Fügenschuh, B. (2017). Exhumation mechanisms of the Tauern Window (Eastern Alps) inferred from Apatite and Zircon fission-track thermochronology. *Tectonics*. doi:10.1002/2016TC004133.

Beucher, R. (2009). *Evolution Néogène de l'arc alpin sud-occidental: Approches sismotectonique et thermochronologique. Géologie appliquée.* Ph.D. dissertation, Université Joseph-Fourier-Grenoble I, France.

Bigot-Cormier F. (2002). *La surrection du massif cristallin externe de l'Argentera (France-Italie) et ses relations avec la déformation pliocène de la marge nord-Ligure: arguments thermochronologiques (traces de fission), géomorphologiques et interprétations de sismique marine*. Ph.D. dissertation, University of Nice, France, 352 pp.

Bistacchi, A., & Massironi, M. (2000). Post-nappe brittle tectonics and kinematic evolution of the north-western Alps: an integrated approach. *Tectonophysics, 327,* 267–292.

Bott, M. H. P. (1959). The mechanisms of oblique slip faulting. *Geological Magazine, 96,* 109–117.

Bousquet, R., Oberhänsli, R., Schmid, S. M., Berger, A., Wiederkehr, M., Robert, C., Möller, A., Rosenberg, C., Zeilinger, G., Molli, G., & Koller, F. (2004). *Metamorphic structure of the Alps. Scale 1:1.000.000*. Paris: Commission for the Geological Map of the World.

Brandon, M. T., Roden-Tice, M. K., & Graver, J. I. (1998). Late Cenozoic exhumation of the Cascadia accretionary wedge in the Olympic Mountains, northwest Washington State. *Geological Society of America Bulletin, 110,* 985–1009.

Brandon, M. T., & Vance, J. A. (1992). New statistical methods for analysis of fission track grain-age distributions with applications to detrital zircon ages from the Olympic subduction complex, western Washington State. *American Journal of Science, 292,* 565–636.

Burg, J. P., Célérier, B., Chaudhry, N. M., Ghazanfar, M., Gnehm, F., & Schnellmann, M. (2005). Fault analysis and paleostress evolution in large strain regions: methodological and geological discussion of the southeastern Himalayan fold-and-thrust belt in Pakistan. *Journal of Asian Earth Sciences, 24,* 445–467.

Bürgi, A., & Klötzli, U. (1990). New data in the evolutionary history of the Ivrea Zone (Northern Italy). *Bulletin der Vereinigung Schweizerische Petroleum-Geologen und Ingenieur, 56,* 49–69.

Campani, M., Mancktelow, D., Seward, D., Rolland, Y., Müller, W., & Guerra, I. (2010). Geochronological evidence for continuous exhumation through the ductile-brittle transition along a crustal-scale low-angle normal fault: Simplon Fault Zone. *Central Alps. Tectonics, 29,* TC3002.

Cardozo, N., & Allmendinger, R. W. (2013). Spherical projections with OSX Stereonet. *Computers and Geosciences, 51,* 193–205.

Carey, E., & Brunier, B. (1974). Analyse théorique et numérique d'un modèle mécanique élémentaire appliqué à l'étude d'une population de failles. *Comptes Rendus de l'Académie des Sciences, 279,* 891–894.

Carpena, J. (1992). Fission track dating of zircon: zircons from Mont Blanc Granite (French-Italian Alps). *The Journal of Geology, 100,* 411–421.

Carpena, J., & Caby, R. (1984). Fission track evidence for late Triassic oceanic crust in the French Occidental Alps. *Geology, 12,* 108–111.

Carpena, J., Pognante, U., & Lombardo, B. (1986). New constraints for the timing of the Alpine metamorphism in the internal ophiolitic nappes from the Western Alps as inferred from fission-track data. *Tectonophysics, 127,* 117–127.

Ceriani, S., Fügenschuh, B., Potel, S., & Schmid, S. M. (2003). Tectono-metamorphic evolution of the frontal Penninic units of the Western Alps: correlation between low-grade metamorphism and tectonic phases. *Schweizerische Mineralogische und Petrographische Mitteilungen, 83,* 111–131.

Cerveny, P. F., Naeser, N. D., Zeitler, P. K., Naeser, C. W., & Johnson, N. M. (1988). History of uplift and relief of the Himalaya during the past 18 million years: Evidence from fission-track ages of detrital zircons from sandstones of the Siwalik Group. In K. L. Kleinspehn & C. Paola (Eds.), *New perspectives in Basin Analysis* (pp. 43–61). New York: Springer.

Champagnac, J. D., Molnar, P., Anderson, R. S., Sue, C., & Delacou, B. (2007). Quaternary erosion-induced isostatic rebound in the Western Alps. *Geological Society of America, 35,* 195–198.

Champagnac, J. D., Sue, C., Delacou, B., & Burkhard, M. (2003). Brittle orogen-parallel extension in the internal zones of the Swiss Alps (south Valais). *Eclogae Geologicae Helveticae, 96,* 325–338.

Champagnac, J. D., Sue, C., Delacou, B., & Burkhard, M. (2004). Brittle deformation in the inner northwestern Alps: from early

orogen-parallel extrusion to late orogen-perpendicular collapse. *Terra Nova, 16,* 232–242.

Champagnac, J. D., Sue, C., Delacou, B., Tricart, P., Allanic, C., & Burkhard, M. (2006). Miocene lateral extrusion in the inner Western Alps revealed by dynamical fault analysis. *Tectonics, 25,* TC3014.

Chéry, J., Genti, M., & Vernant, P. (2016). Ice cap melting and low-viscosity crustal root explain the narrow geodetic uplift of the Western Alps. *Geophysical Research Letters, 43,* 3193–3200.

Ciancaleoni, L. (2005). *Deformation processes during the last stages of the continental collision: the brittle-ductile fault systems in the Bergell and Insubric areas (Eastern Central Alps)*. Ph.D. dissertation, Université de Neuchâtel, Switzerland.

Ciancaleoni, L., & Marquer, D. (2008). Late Oligocene to early Miocene lateral extrusion at the eastern border of the Lepontine Dome of the central Alps (Bergell and Insubric areas, eastern central Alps). *Tectonics, 27,* TC4008.

Collombet, M., Thomas, J. C., Chauvin, A., Tricart, P., Bouillin, J. P., & Gratier, J. P. (2002). Counterclockwise rotation of the western Alps since the Oligocene: new insights from paleomagnetic data. *Tectonics, 21,* 352–366.

De Graciansky, P. C., Robert, R. D., & Tricart, P. (2011). *The Western Alps, from rift to passive margin to orogenic belt: an integrated geoscience overview* (p. 432). Amsterdam: Elsevier.

Decker, K., Meschede, M., & Ring, U. (1993). Fault slip analysis along the northern margin of the Eastern Alps (Molasse, Helvetic nappes, North and South Penninic flysch, and the Northern Calcareous Alps). *Tectonophysics, 223,* 291–312.

Delacou, B., Sue, C., Champagnac, J. D., & Burkhard, M. (2005). Origin of the current stress field in the Western/Central Alps: role of gravitational reequilibration constrained by numerical modelling. In D. Gapais, J. P. Brun, & P. R. Cobbold (Eds.), *Deformation, rheology and tectonic: from minerals to the lithosphere* (pp. 295–310). London: Geological Society Special publication (London).

Dewey, J.F., Helman, M.L., Turco, E., Hutton, D.H.W. & Knott, S.D. (1989). Kinematics of the western Mediterranean. In Coward, M.P., Dietrich, D., Park, R.G. (Eds.). *Alpine tectonics, Geological Society Special Publication (London), 45*, 265-283.

Dewey, J. F., Pitman, W. C. I., Ryan, W. B. F., & Bonnin, J. (1973). Plate tectonics and the evolution of the Alpine system. *Bulletin of the Geological Society of America, 84,* 137–180.

Diaz, J., Gil, A., & Gallart, J. (2013). Uppermost mantle seismic velocity and anisotropy in the Euro-Mediterranean region from *Pn* and *Sn* tomography. *Geophysical Journal International, 192,* 310–325.

Dodson, M. H. (1973). Closure temperature in cooling geochronological and petrological systems. *Contribution to Mineralogy and Petrology, 40,* 259–274.

Doglioni, C. (1991). A proposal for the kinematic modelling of W-dipping subductions—possible applications to the Tyrrhenian-Apennines system. *Terra Nova, 3,* 423–434.

Dunkl, I., Frisch, W., & Grundmann, G. (2003). Zircon fission track thermochronology of the south-eastern part of the Tauern Window and the adjacent Austroalpine margin, Eastern Alps. *Eclogae Geologicae Helveticae, 96,* 209–217.

Elias, J. (1998). The thermal history of the Ötztal-Stubai complex (Tyrol, Austria/Italy) in the light of the lateral extrusion model. *Tübinger Geowissenchaftliche Arbeiten, Reihe A., 42,* 172.

Faccenna, C., Becker, T. W., Auer, L., Billi, A., Boschi, L., Brun, J. P., Capitano, F.A., Funiciello, F., Horvath, F., Jolivet, L., Piromallo, C., Royden, L., Rossetti, F., & Serpelloni, E. (2014). Mantle dynamics in the Mediterranean. *Reviews of Geophysics*, *52*, 283–332. doi:10.1002/2013RG000444.

Faccenna, C., Piromallo, C., Crespo-Blanc, A., Jolivet, L., & Rossetti, F. (2004). Lateral slab deformation and the origin of the western Mediterranean arcs. *Tectonics, 23,* TC1012.

Flisch, M. (1986). Die Hebungsgeschichte der oberostalpinen Silvretta-Decke seit der mittleren Kreide. *Bulletin der Vereinigung Schweizerischer Petroleum-Geologen und Ingenieure, 53,* 23–49.

Fox, M., Herman, F., Kissling, E., & Willett, S. D. (2015). Rapid exhumation in the Western Alps driven by slab detachment and glacial erosion. *Geology, 43,* 379–382.

Fox, M., Herman, F., Willett, S. D., & Schmid, S. M. (2016). The exhumation history of the European Alps inferred from linear inversion of thermochronometric data. *American Journal of Science, 316,* 505–541.

Frank, W. (1987). Evolution of the Austrolapine elements in the Cretaceous. In W. Frank, H. Flügel, & P. Faupl (Eds.), *Geodynamics of the Eastern Alps* (pp. 379–406). Vienna: Deuticke.

Frisch, W. (1979). Tectonic progradation and plate tectonic evolution of the Alps. *Tectonophysics, 60,* 121–139.

Froitzheim, N., Schmid, S. M., & Frey, M. (1996). Mesozoic paleogeography and the timing of eclogite facies metamorphism in the Alps: a working hypothesis. *Eclogae Geologicae Helveticae, 89,* 81–110.

Fügenschuh, B. (1995). *Thermal and Kinematic History of the Brenner Area (Eastern Alps, Tyrol).* Ph.D. dissertation, ETH Zürich 1995, Zürich, Switzerland, 225 pp.

Fügenschuh, B., Loprieno, A., Ceriani, S., & Schmid, S. M. (1999). Structural analysis of the Subbriançonnais and Valais units in the area of Moûtiers (Savoy, Western Alps). Palaeographical and tectonic consequences. *International Journal of Earth Sciences, 88,* 201–218.

Fügenschuh, B., & Schmid, S. M. (2003). Late stages of deformation and exhumation of an orogen constrained by fission-track data: a case study in the Western Alps. *Geological Society of America Bulletin, 15,* 1425–1440.

Fügenschuh, B., Seward, D., & Mantckelow, N. S. (1997). Exhumation in a convergent orogen: the western Tauern Window. *Terra Nova, 9,* 213–217.

Garver, J. I., Reiners, P. R., Walker, L. J., Ramage, J. R., & Perry, S. E. (2005). Implications for timing of Andean uplift based on thermal resetting of radiation-damaged zircon in the Cordillera Huayhuash, northern Perú. *The Journal of Geology, 113,* 117–138.

Gephart, J. W. (1990). Stress and the direction of slip on fault planes. *Tectonics, 9,* 845–858.

Gidon, M. (1974). L'arc alpin a-t-il une origine tourbillonnaire? *Comptes Rendus de l'Académie des Sciences, 278,* 21–24.

Grosjean, G., Sue, C., & Burkhard, M. (2004). Late Neogene extension in the vicinity of the Simplon fault zone (central Alps, Switzerland). *Eclogae Geologicae Helveticae, 97,* 33–46.

Handy, M. R., Favaro, S., Schmid, S. M., & Bertrand, A. (2013). Modes of orogen-parallel stretching and extensional exhumation in response to microplate indentation and roll-back subduction (Tauern Window, Eastern Alps). *International Journal of Earth Sciences, 102*(6), 1627–1654. doi:10.1007/s00531-013-0894-4.

Handy, M. R., Schmid, S. M., Bousquet, R., Kissling, E., & Bernoulli, D. (2010). Reconciling plate-tectonic reconstructions of Alpine Tethys with the geological–geophysical record of spreading and subduction in the Alps. *Earth-Science Reviews, 102,* 121–158.

Heberer, B., Reverman, B. L., Fellin, M. G., Neubauer, F., Dunkl, I., Zattin, M., Seward, D., Genser, J., & Brack, P. (2016). Postcollisional cooling history of the Eastern and Southern Alps and its linkage to Adria indentation. *International Journal of Earth Sciences*. doi:10.1007/s00531-016-1367-3.

Hejl, E., & Wagner, G. (1991). Spaltspuren in Apatit und Zirkon-Schlüssel zur Niedertemperatur- und Hebungsgeschichte der Alpen. *Schweizerische Mineralogische und Petrographische Mitteilungen, 71,* 63–71.

Hetzel, R., Altenberger, U., & Strecker, M. R. (1996). Structural and chemical evolution of pseudotachylites during seismic events. *Mineralogy and Petrology, 58,* 33–50.

Hintersberger, E., Thiede, R. C., & Strecker, M. R. (2011). The role of extension during brittle deformation within the NW Indian Himalaya. *Tectonics, 30,* TC3012.

Hurford, A. J., & Hunziker, J. C. (1985). Alpine cooling history of the Monte Mucrone eclogites. *Schweizerische Mineralogische und Petrographische Mitteilungen, 65,* 325–334.

Hurford, A. J., & Hunziker, J. C. (1989). A revised thermal history for the Gran Paradiso massif. *Schweizerische Mineralogische und Petrographische Mitteilungen, 69,* 319–329.

Jolivet, L., Augier, R., Faccenna, C., Negro, F., Rimmele, G., Agard, P., Robin, C., Rossetti, F., & Crespo-Blanc, A. (2008). Subduction, convergence and the mode of backarc extension in the Mediterranean region. *Bulletin de la Société Géologique de France, 179*, 525–550. doi:10.2113/gssgfbull.179.6.525.

Kasuya, M., & Naeser, C. W. (1988). The effect of α-damage on fission-track annealing in zircon. International journal of radiation applications and instrumentation part D. *Nuclear Tracks and Radiation Measurements, 14,* 477–480.

Keller, L. M., Hess, M., Fügenschuh, B., & Schmid, S. (2005). Structural and metamorphic evolution of the Camughera-Moncucco, Antrona and Monte Rosa units southwest of the Simplon line, Western Alps. *Eclogae Geologicae Helveticae, 98,* 19–49.

Kralik, M., Clauer, N., Holnsteiner, R., Huemer, H., & Kappel, F. (1992). Recurrent fault activity in the Grimsel test site (GTS, Switzerland), revealed by Rb–Sr, K-Ar and tritium isotope techniques. *Journal of the Geological Society, London, 149,* 293–301.

Kralik, M., Klima, K., & Riedmüller, G. (1987). Dating fault gouges. *Nature, 327,* 315–317.

Lacombe, O. (2012). Do fault slip data inversions actually yield "paleostresses" that can be compared with contemporary stresses? A critical discussion. *Comptes Rendus Geoscience, 344,* 159–173.

Laubscher, H. (1985). Large scale, thin skinned thrusting in the Southern Alps : kinematic models. *Geological Society of America Bulletin, 96,* 710–718.

Laubscher, H. (1996). Shallow and deep rotations in the Miocene Alps. *Tectonics, 15,* 1022–1035.

Luth, S. (2011). *Orogenesis and Subduction in Analogue Models, Expressions of Subduction Polarity Change below the Alps*. Ph.D. dissertation, Vrije Universiteit Amsterdam, Netherland.

Lyons, J. B., & Snellenberg, J. (1971). Dating faults. *Geological Society of America Bulletin, 82,* 1749–1752.

Mancktelow, N. S. (1985). The Simplon Line: a major displacement zone in the western Lepontine Alps. *Eclogae Geologicae Helveticae, 78,* 73–96.

Mancktelow, N. S., Stöckli, D. F., Grollimund, B., Müller, W., Fügenschuh, F., Viola, G., Seward, D., & Villa, I. M. (2001). The DAV and Periadriatic fault systems in the Eastern Alps south of the Tauern Window. *International Journal of Earth Sciences, 90,* 593–622. doi:10.1007/s005310000190.

Marrett, R., & Allmendinger, R. W. (1990). Kinematic analysis of fault-slip data. *Journal of Structural Geology, 12,* 973–986.

Martin, S., Godard, G., Laurenzi, M. A., & Vigano, A. (2016). Pseudotachylytes of the Tonale nappe (Italian Alps): petrogenesis, ^{40}Ar-^{39}Ar geochronology and tectonic implications. *Italian Journal of Geoscience, 135,* 217–235.

McDougall, I., & Harrison, M. T. (1999). *Geochronology and Thermochronology by the 40Ar/39Ar Method* (p. 269). Oxford: Oxford University Press.

Michalski, I., & Soom, M. (1990). The Alpine thermo-tectonic evolution of the Aar and Gotthard massifs, Central Switzerland: fission-Track ages on zircons and apatites and K-Ar mica ages. *Schweizerische Mineralogische und Petrographische Mitteilungen, 70,* 373–387.

Milnes, A. G. (1978). Structural zones and continental collision, Central Alps. *Tectonophysics, 47,* 369–392.

Molli, G., Crispini, L., Malusà, M., Mosca, P., Piana, F. & Federico, L. (2010). Geology of the Western Alps-Northern Apennine junction area: a regional review. In Beltrando, M., Peccerillo, A., Mattei, M., Conticelli, S., Doglioni, C. (Eds.), *The Geology of Italy: tectonics and life along plate margins, Journal of the Virtual Explorer, Electronic Edition,* ISSN 1441-8142, 36, doi:10.3809/jvirtex.(2010).00215.

Most, P. (2003). *Late Alpine cooling histories of tectonic blocks along the central part of the Transalp-Traverse (Inntal-Gadertal): constraints from geochronology*. Ph.D. dissertation, University of Tübingen, Germany, pp. 97.

Müller, W., Mancktelow, N. S., & Meier, M. (2000). Rb-Sr microchrons of synkinematic mica in mylonites: an example from the DAV fault of the Eastern Alps. *Earth and Planetary Science Letters, 180,* 385–397.

Müller, W., Prosser, G., Mancktelow, N. S., Villa, I. M., Kelley, S. P., Viola, G., & Oberli, F. (2001). Geochronological constraints on the evolution of the Periadriatic Fault System (Alps). *International Journal of Earth Sciences, 90*, 623–653. doi:10.1007/s005310000187.

Nemes, F. (1996). *Kinematics of the Periadriatic Fault in the Eastern Alps-evidence from structural analysis, fission track dating and basin modelin*. Ph.D. thesis, pp. 225. Univ. of Salzburg, Salzburg, Austria,1996.

Nocquet, J. M., Sue, C., Walpersdorf, A., Tran, T., Lenôtre, N., Vernant, P., Cushing, M., Jouanne, F., Masson, F., Baize, S., Chéry, J., & van der Beek, P.A. (2016). Present-day uplift of the western Alps. *Nature Science Report*. doi:10.1038/srep28404.

Peresson, H., & Decker, K. (1997). Far-field effects of late Miocene subduction in the Eastern Carpathians: e-W compression and inversion of structures in the Alpine-Carpathian-Pannonian region. *Tectonics, 16,* 38–56.

Perrone, G., Cadoppi, P., Balestro, G., & Tallone, S. (2011). Post-collisional tectonics in the Northern Cottian Alps (italian Western Alps). *International Journal of Earth Sciences, 100,* 1349–1373.

Petit, J. P. (1987). Criteria for the sense of movement on fault surfaces in brittle rocks. *Journal of Structural Geology, 9,* 597–608. doi:10.1016/0191-8141(87)90145-3.

Pfiffner, O. A., & Burkhard, M. (1987). Determination of paleostress axis orientations from fault, twin and earthquake data. *Annales Tectonicae, 1*(1), 48–57.

Platt, J. P. (1986). Dynamic of orogenic wedges and the uplift of high pressure metamorphic rocks. *Geological Society of America Bulletin, 97,* 1037–1053.

Pomella, H., Klötzli, U., Scholger, R., Stipp, M., & Fügenschuh, B. (2011). The Northern Giudicarie and the Meran-Mauls fault (Alps, Northern Italy) in the light of new paleomagnetic and geochronological data from boudinaged Eo-/Oligocene tonalities. *International Journal of Earth Sciences, 100*(8), 1827–1850.

Pomella, H., Stipp, M., & Fügenschuh, B. (2012). Thermochronological record of thrusting and strike-slip faulting along the Giudicarie fault system (Alps, Northern Italy). *Tectonophysics, 579,* 118–130.

Qorbani, E., Bianchi, I., & Bokelmann, G. (2015a). Slab detachment under the Eastern Alps seen by seismic anisotropy. *Earth and Planetary Science Letters, 409,* 96–108.

Qorbani, E., Kurz, W., Bianchi, I., & Bokelmann, G. (2015b). Correlated crustal and mantle deformation in the Tauern Window, Eastern Alps. *Austrian Journal of Earth Sciences, 108,* 161–173.

Rabin, M., Sue, C., Valla, P. G., Champagnac, J. D., Carry, N., Bichet, V., Eichenberger, U., & Mudry, J. (2015). Deciphering neotectonics from river profile analysis in the karst Jura Mountains (northern Alpine foreland). *Swiss Journal of Geosciences, 108,* 401–424. doi:10.1007/s00015-015-0200-5.

Ratschbacher, L., Frisch, W., & Linzer, H. G. (1991a). Lateral extrusion in the Eastern Alps: part II. *Structural analysis. Tectonics, 10,* 257–271.

Ratschbacher, L., Frisch, W., Neubauer, F., Schmid, S. M., & Neugebauer, J. (1989). Extension in compressional orogenic belts: the Eastern Alps. *Geology, 17,* 404–407.

Ratschbacher, L., Merle, O., Davy, P., & Cobbold, P. (1991b). Lateral extrusion in the Eastern Alps, Part. 1: boundary conditions and experiments scaled for gravity. *Tectonics, 10,* 245–256.

Reverman, R., Fellin, M. G., Herman, F., Willet, S. D., & Fitoussi, C. (2012). Climatically versus tectonically forced erosion in the Alps: thermochronometric constraints from the Adamello Complex, Southern Alps, Italy. *Earth and Planetary Science Letters, 339–340,* 27–138.

Riedel, W. (1929). *Zur Mechanik geologischer Brucherscheinungen, ein Beitrag zum Problem der Fiederspalten* (pp. 354–368). Geologie und Paleontologie B: Zentralblatt fur Mineralogie.

Rolland, Y., Cox, C. F., & Corsini, M. (2009). Constraining deformation stages in brittle–ductile shear zones from combined field mapping and 40Ar/39Ar dating: the structural evolution of the Grimsel Pass area (Aar Massif, Swiss Alps). *Journal of Structural Geology, 31,* 1377–1394.

Rosenberg, C. L., Berger, A., Belahsen, N., & Bousquet, R. (2015). Relating orogen width to shortening, erosion, and exhumation during Alpine collision. *Tectonics, 34,* 1306–1328.

Rosenberg, C. L., Brun, J.-P., Cagnard, F., & Gapais, D. (2007). Oblique indentation in the Eastern Alps: Insights from laboratory experiments. *Tectonics, 26,* TC2003.

Rosenberg, C. L., Brun, J.-P., & Gapais, D. (2004). Indentation model of the Eastern Alps and the origin of the Tauern Window. *Geology, 32,* 997–1000.

Royden, L. H. (1993). The tectonic expression slab pull at continental convergent boundaries. *Tectonics, 12,* 303–325.

Sachsenhofer, R.F., Lankreijer, A., Cloething, S., & Ebner, F. (1997). Subsidence analysis and quantitative basin modeling in the Styrian basin (Pannonian Basin system, Austria), *Tectonophysics*, *272*, 175–196.

Schlunegger, F., & Kissling, E. (2015). Slab rollback orogeny in the Alps and evolution of the Swiss Molasse basin. *Nature Communications*. doi:10.1038/ncomms9605.

Schlunegger, F. & Willett, S. (1999). Spatial and temporal variations in exhumation of the central Swiss Alps and implications for exhumation mechanisms. In U. Ring, M.T. Brandon, G. Lister, S.D. Willett (Eds.), *Exhumation Processes: Normal Faulting, Ductile Flow and Erosion, edited by Geological Society Special publication (London), 154*, 157–179.

Schmid, S., & Froitzheim, N., (1993). Oblique slip and blockrotation along the Engadine line. *Eclogae Geologicae Helvetiae*, *86*, 569–593.

Schmid, S. M., Fügenschuh, B., Kissling, E., & Schuster, R. (2004). Tectonic map of the Alps and overall architecture of the alpine orogen. *Eclogae geologicae Helveticae, 97,* 93–117.

Schmid, S. M., & Kissling, E. (2000). The arc of the western Alps in the light of geophysical data on deep crustal structure. *Tectonics, 19,* 62–85.

Schmid, S., Kissling, E., Diehl, T., VanHinsbergen, D., & Molli, G. (2017). Ivrea mantle, wedge arc of the Western Alps, and kinematic evolution of the Alps-Apeninnes orogenic system. *Swiss Journal of Geosciences*. doi:10.1007/s00015-016-0237-0.

Schmid, S. M., Pfiffner, O. A., Froitzheim, N., Schönborn, G., & Kissling, E. (1996). Geophysical-geological transect and tectonic evolution of the Swiss-Italian Alps. *Tectonics, 15,* 1036–1064.

Schuster, R. (2015). Zur Geologie der Ostalpen. *Abhandlungen der Geologischen Bundesanstalt, 64,* 143–165.

Schwartz, S. (2000). *La zone piémontaise des Alpes occidentales: un paléo-complexe de subduction. Arguments métamorphiques, géochronologiques et structuraux*. Ph.D. dissertation, University of Lyon 1, France, 341 pp.

Selverstone, J. (1988). Evidence for east-west crustal extension in the Eastern Alps: implications for the unroofing history of the Tauern Window. *Tectonics, 7,* 87–105.

Sengör, A. M. C. (1979). Mid-Mesozoic closure of Permo-Triassic Tethys and its implications. *Nature, 279,* 590–593.

Seward, D., Ford, M., Bürgisser, J., Lickorish, H., Williams, E. A., & Meckel, L. D. (1999). Preliminary results of fission track analyses in the Southern Pelvoux area, SE France. *Memorie di Scienze Geologiche Padova, 51,* 25–31.

Seward, D., & Mancktelow, N. S. (1994). Neogene kinematics of the central and Western Alps: evidence from fission-track dating. *Geology, 22,* 803–806.

Soom, M.A. (1990). *Abkühlungs- und Hebungsgeschichte der Externmassive und der penninischen Decken beidseits der Simplon-Rhone-Linie seit dem Oligozän: Spaltspurdatierung and Apatit/Zirkon und K-Ar-Datierungen an Biotit/Muskovit (westliche Zentralalpen)*. Ph.D. dissertation, University of Bern, Switzerland, 64 pp.

Spada, M., Bianchi, I., Kissling, E., Piana, Agostinetti N., & Wiemer, S. (2013). Combining controlled-source seismology and receiver function information to derive 3-D Moho topography for Italy. *Geophysical Journal International, 194,* 1050–1068.

Sperner, B., Ratschbacher, L., & Nemcok, M. (2002). Interplay between subduction retreat and lateral extrusion: tectonics of the Western Carpathians. *Tectonics, 21,* 1–24.

Sperner, B., Ratschbacher, L., & Ott, R. (1993). Fault-striae analysis: a Turbo pascal program for graphical presentation and reduced stress tensor calculation. *Computers & Geosciences, 19,* 1361–1388.

Spray, J. G. (1992). A physical basis for the frictional melting of some rock- forming minerals. *Tectonophysics, 204,* 205–221.

Stampfli, G. M., Mosar, J., Marquer, D., Marchant, R., Baudin, T., & Borel, G. (1998). Subduction and obduction processes in the Swiss Alps. *Tectonophysics, 296,* 159–204.

Steck, A. (1980). Deux directions principales de flux synmétamorphique dans les Alpes centrales. *Bulletin de la Société Vaudoise de Science naturelle, 75,* 141–149.

Steenken, A., Siegesmund, S., Heinrichs, T., & Fügenschuh, B. (2002). Cooling and exhumation of the Rieserferner Pluton (Eastern Alps). *International Journal of Earth Sciences, 91,* 799–817.

Stipp, M., Stünitz, H., Heilbronner, R., & Schmid, S. M. (2002). The eastern Tonale fault zone: a "natural laboratory" for crystal plastic deformation of quartz over a temperature range from 250 to 700 °C. *Journal of Structural Geology, 24,* 1861–1884. doi:10.1016/S0191-8141(02)00035-4.

Stöckhert, B. (1991). Constraints on the late thermotectonic evolution of the Western Alps: evidence for episodic rapid uplift. *Tectonics, 10,* 758–769.

Sue, C. (1998). *Dynamique actuelle et récente des Alpes occidentales internes–approche structurale et sismologique*. Ph.D. dissertation, Université Joseph Fourier, Grenoble, France.

Sue, C., Delacou, B., Champagnac, J. D., Allanic, C., Tricart, P., & Burkhard, M. (2007). Extensional neotectonics around the bend of the western/central Alps: an overview. *International Journal of Earth Sciences, 96,* 1101–1129. doi:10.1007/s00531-007-0181-3.

Sue, C., Thouvenot, F., Fréchet, J., & Tricart, P. (1999). Widespread extension in the core of the western Alps revealed by earthquake analysis. *Journal of Geophysical Research, 104,* 25611–25622.

Sue, C., & Tricart, P. (1999). Late-Alpine brittle extension above the Frontal Pennine thrust near Briançon, western Alps. *Eclogae Geologicae Helveticae, 92,* 171–181.

Sue, C., & Tricart, P. (2002). Widespread post-nappe normal faulting in the Internal western Alps: a new constraint on arc dynamic. *Journal of the Geological Society of London, 159,* 61–70.

Sue, C., & Tricart, P. (2003). Neogene to ongoing normal faulting in the inner western Alps: a major evolution of the late alpine tectonics. *Tectonics, 22,* 1–25.

Tapponnier, P. (1977). Evolution tectonique du système alpin en Méditerranée: poinçonnement et écrasement rigide plastique. *Bulletin de la Société Géologique de France, 7,* 437–460.

Termier, P. (1903). Les nappes des Alpes orientales et la synthèse des Alpes. *Bulletin de la Société Géologique de France, 3,* 711–766.

Thomas, J. C., Claudel, M. E., Collombet, M., Dumont, T., Tricart, P., & Chauvin, A. (1999). First paleomagnetic data from the sedimentary cover of the French penninic Alps: evidence for Tertiary counterclockwise rotations in the western Alps. *Earth and Planetary Science Letters, 171,* 561–574.

Tollmann, A. (1963). *Ostalpensynthese* (p. 256). Wien: Deuticke.

Tricart, P. (1984). From passive margin to continental collision: a tectonic scenario for the Western Alps. *American Journal of Science, 284,* 97–120.

Turner, F. J. (1953). Nature and dynamic interpretation of deformation lamellae in calcite of three marbles. *American Journal of Science, 251,* 276–298.

Twiss, R. J., & Unruh, J. R. (1998). Analysis of fault slip inversions: do they constrain stress or strain rate? *Journal of Geophysical Research Solid Earth, 103,* 12205–12222.

Van der Pluijm, B. A., Hall, C. M., Vrolijk, P. J., Pevear, D. R., & Covey, M. C. (2001). The dating of shallow faults in the Earth's crust. *Nature, 412,* 172–175.

Vernant, P., Hivert, F., Chéry, J., Steer, P., Cattin, R., & Rigo, A. (2013). Erosion-induced isostatic rebound triggers extension in low convergent mountain ranges. *Geology, 41,* 467–470.

Vialon, P., Rochette, P. & Ménard, G. (1989). Indentation and rotation in the Alpine arc. In M.P. Coward, D. Dietrich, R.G. Park (Eds.), *Alpine tectonics, Geological Society Special publication (London)* 45, 329–338).

Viola, G., Mancktelow, N. S., & Seward, D. (2001). Late Oligocene-Neogene evolution of Europe-Adria collision: new structural and geochronological evidence from the Giudicarie fault system (Italian Eastern Alps). *Tectonics, 20,* 999–1020.

Von Blanckenburg, F. (1992). Combined high-precision chronometry and geochemical tracing using accessory minerals: applied to the Central-Alpine Bergell Intrusion (Central Europe). *Chemical Geology, 100,* 19–40.

Von Blanckenburg, F., & Davies, J. H. (1995). Slab breakoff—a model for syncollisional magmatism and tectonics in the Alps. *Tectonics, 14,* 120–131.

Wallace, R. E. (1951). Geometry of shearing stress and relation to faulting. *The Journal of Geology, 59,* 118–130.

Walpersdorf, A., Sue, C., Baize, S., Cotte, N., Bascou, P., Beauval, C., Collard, P., Daniel, G., Dyer, H., Grasso, J-R., Hautecoeur, O., Helmstetter, A., Hok, S., Langlais, M., Menard, G., Moussavi, Z., Ponton, F., Rizza, M., Rolland, L., Souami, D., Thirard, L., Vaudey, P., Voisin, C., & Martinod, J. (2015). Coherence between geodetic and seismic deformation in a context of slow tectonic activity (SW Alps, France). *Journal of Geodynamics, 85,* 58–65. doi:10.1016/j.jog.2015.02.001.

Wang, X., & Neubauer, F. (1998). Orogen-parallel strike-slip faults bordering metamorphic core complexes: the Salzach-Enns fault zone in the Eastern Alps. *Journal of Structural Geology, 20,* 799–818.

Weh, M., & Froitzheim, N. (2001). Penninic cover nappes in the Prättigau half-window (Eastern Switzerland): structure and tectonic evolution. *Eclogae Geologicae Helveticae, 94,* 237–252.

Willett, S. D., Schlunegger, F., & Picotti, V. (2006). Messinian climate change and erosional destruction of the central European Alps. *Geology, 34,* 613–616.

Wölfler, A., Dekant, C., Danisìk, M., Kurz, W., Dunkl, I., Putis, M., & Frisch, W. (2008). Late stage differential exhumation of crustal blocks in the central Eastern Alps: evidence from fission track and (U–Th)/He thermochronology. *Terra Nova, 20,* 378–384.

Yamada, R., Tagami, T., Nishimura, S., & Ito, H. (1995). Annealing kinematics of fission tracks in zircon: an experimental study. *Chemical Geology (Isotope Geoscience Section), 122,* 249–258.

Yamaji, A. (2000). The multiple inverse method: a new technique to separate stresses from heterogeneous fault-slip data. *Journal of Structural Geology, 22,* 441–452.

Zanchetta, S., D'Adda, P., Zanchi, A., & Maria Villa, I. (2011). Cretaceous-Eocene compression in the central Southern Alps (N Italy) inferred from $^{40}Ar/^{39}Ar$ dating of pseudotachylytes along regional thrust faults. *Journal of Geodynamics, 51,* 245–263.

Zattin, M., Cuman, A., Fantoni, R., Martin, S., Scotti, P., & Stefani, C. (2006). From Middle Jurassic heating to Neogene cooling: the thermochronological evolution of the southern Alps. *Tectonophysics*, *414*, 191–202.

Zattin, M., Stefani, C., & Martin, S. (2003). Detrital fission-track analysis and sedimentary petrofacies as keys of alpine exhumation: the example of the Venetian Foreland (European Southern Alps, Italy). *Journal of Sedimentary Research, 73,* 1051–1061.

Zhao, L., Paul, A., Guillot, S., Solarino, S., Malusa, M. G., Zheng, T., et al. (2015). First seismic evidence for continental subduction beneath the Western Alps. *Geology, 43,* 815–818.

Zwingmann, H., & Mancktelow, N. (2004). Timing of Alpine fault gouge. *Earth and Planetary Science Letters, 223,* 415–425.